PCCP

Molecular Dynamics Simulations Demonstrate That Nonideal Mixing Dominates Subsaturation Organic Aerosol Hygroscopicity

Journal:	*Physical Chemistry Chemical Physics*
Manuscript ID	CP-ART-01-2021-000245.R1
Article Type:	Paper
Date Submitted by the Author:	29-Mar-2021
Complete List of Authors:	Roston, Daniel; University of California San Diego, Chemistry & Biochemistry

Molecular Dynamics Simulations Demonstrate That Nonideal Mixing Dominates Subsaturation Organic Aerosol Hygroscopicity

Daniel Roston*

Department of Chemistry and Biochemistry, University of California-San Diego, La Jolla, CA 92093

*droston@ucsd.edu

Abstract

The microscopic properties that determine hygroscopic behavior are complex. The importance of hygroscopicity to many areas, and particularly atmospheric chemistry, in terms of aerosol growth and cloud nucleation, mandate the need for robust models to understand this behavior. Toward this end, we have employed molecular dynamics simulations to calculate hygroscopicity from atomistic models using free energy perturbation. We find that currently available force fields may not be well-suited to modeling the extreme environments of aerosol particles. Nonetheless, the results illuminate some shortcomings in our current understanding of hygroscopic growth and cloud nucleation. The most widely used model of hygroscopicity, κ-Köhler Theory (κKT), breaks down in the case of deviations from ideal solution behavior and empirical adjustments within the simplified framework cannot account for non-ideal behavior. A revised model that incorporates non-ideal mixing rescues the general framework of κKT and allows us to understand our simulation results as well as the behavior of atmospheric aerosols over the full range of humidity. The revised model shows that non-ideal mixing dominates hygroscopic growth at subsaturation humidity. Thus, a model based on ideal mixing will fail to predict subsaturation growth from cloud condensation nucleus (CCN) activation or *vice versa*; a single parameter model for hygroscopicity will generally be insufficient to extrapolate across wide ranges of humidity. We argue that in many cases, when data are limited to subsaturation humidity, an empirical model for non-ideal mixing may be more successful than one for ideal mixing.

Introduction

Certain substances absorb water from humid surroundings and their tendency to do so, referred to as hygroscopicity, affects phenomena ranging from cloud formation to drug shelf-life to viral transmission. Predictive models of hygroscopicity have been a long-sought goal especially in atmospheric chemistry because the hygroscopicity of aerosol particles indicates their ability to serve as cloud condensation nuclei (CCN).[1] Prediction of CCN activity by aerosols of different composition is necessary for models of weather and climate as well as for modeling the transport of those aerosols through the atmosphere. Water uptake also affects the integrity of manufactured goods, such as pharmaceuticals. Hence, predictive models of water uptake would allow chemists to consider hygroscopicity in rational drug design and fabrication of other materials that require stability in potentially humid environments. Furthermore, the (de)hydration of airborne viral

aerosols and droplets affects their lifetime and diffusivity through air, which can affect disease transmission.[2] Thus, robust models of water uptake and hygroscopicity would be useful in a wide range of applications.

Hygroscopicity for a given substance is typically measured under two different relative humidity regimes: subsaturation humidity (0 to 100% relative humidity) and supersaturation humidity (> 100% relative humidity). In the subsaturation humidity regime, one can measure hygroscopic growth factors, defined as the ratio of the hydrated diameter (D) of the particle to its dry diameter (D_d). A second approach is to measure the critical supersaturation (S_c), which is the supersaturation at which CCN activation occurs. In principle, hygroscopic behavior is governed by the general framework of Köhler Theory, which allows measurements in one environment and for one particle size to predict the behavior of particles of different sizes and in different environments. Köhler Theory connects hygroscopic growth and CCN activation of a particle to its surrounding humidity through a combination of the activity of water in the particle and the effects of the curvature of the particle. In its most basic form, though, Köhler Theory lacks quantitatively predictive capabilities. The need for simple, reliable, and predictive models of aerosol behavior has sparked a great deal of recent interest in measurements of hygroscopicity and an attempt to understand how Köhler Theory might be made to conform to measurements. So far, the results have been mixed, with gaps remaining in our ability to use the framework of Köhler Theory in a quantitatively accurate way.

The desire for more predictive models inspired us to develop a computational method to determine hygroscopicity from atomistic models. To do so, we have used molecular dynamics (MD) simulations and free energy methods to determine how solutes affect the free energy of adding water to a particle, in terms of the chemical potential of water. The importance of hygroscopicity to atmospheric chemistry made us focus specifically on the chemical potential of water in aerosol particles, but the strategy can also be applied to bulk. We attempted to interpret the free energy simulation results in the context of a widely used version of Köhler Theory, referred to as κ-Köhler Theory (κKT).[3] The most simplified form of κKT uses a single solute-dependent parameter (κ) to model the activity of water. Limitations of the single parameter treatment have inspired elaborations of the model that account for solubility,[4] surface partitioning,[5] and non-ideal mixing,[6] but gaps remain in our ability to extrapolate hygroscopic growth over large ranges of

humidity and especially to use hygroscopic growth at subsaturation humidity to predict CCN activation.[6-10]

The limitations of κKT are laid strikingly bare by the results from our MD simulations. In particular, we find that non-ideal mixing and especially positive excess free energy of mixing (positive deviations from Raoult's law) pose a devastating challenge to simplified κKT. However, by incorporation of excess free energy of mixing using a single additional solute-dependent parameter, we are able to overcome this challenge. We explore here how a model that includes non-ideal mixing predicts hygroscopic growth at sub- and super-saturation humidity. We find that non-ideal mixing tends to be more important at low humidity[6] where solute concentration is highest. In fact, the excess free energy of mixing tends to dominate the overall free energy of mixing at high solute concentration, particularly for organic solutes. Neglect of the non-ideal components of mixing will generally be hazardous. Moreover, in some cases where data are limited, a model that addresses the excess free energy of mixing (while neglecting the ideal component) may achieve greater predictive ability. Non-ideal mixing can greatly suppress or enhance growth at low humidity without necessarily altering S_c for that particle. This may in fact explain the inability of simple κKT to extrapolate from subsaturation growth factors to measured S_c or vice versa.[7, 9, 10] A model that includes the effect of non-ideal mixing may solve what has become known as the "hygroscopicity gap", where certain solutes with limited subsaturation growth factors tend to have higher than expected CCN activity. While κKT is attractive in terms of its simplicity, particularly for mixtures of multiple solutes, its limitations in accurately reflecting aerosol behavior require that we progress from a model that assumes concentrated solutions of water behave ideally.

Theory

κ -Köhler Theory: The Ideal Limit

For nearly a century, Köhler theory has provided a framework for understanding water uptake by aerosols, measured by changes in particle diameter (D) as a function of humidity. In this framework, the relative humidity, or "saturation ratio", S, over an aqueous droplet is a function of diameter, composed of two factors:

$$S(D) = a_w \exp\left(\frac{A}{D}\right) \qquad (1)$$

Where

$$A = \frac{4\sigma M_w}{RT\rho_w} \qquad (2)$$

In these expressions, a_w is the activity of water in the droplet, and the exponential is the Kelvin factor, which accounts for the curvature of the droplet in terms of the surface tension (σ), the molecular weight and density of water (M_w and ρ_w, respectively), and the diameter of the particle. R is the gas constant and T is the temperature. Eq. 1 can explain hygroscopic growth as a function of humidity and the function reaches a maximum that corresponds to S_c, the supersaturation at which CCN activation occurs. The model accounts for a great deal of phenomena, but historically, determining a_w required a number of solute-specific parameters, including its molar mass, density, molality, etc., which are often unknown for environmentally important aerosols.

In a remarkably useful simplification of Köhler theory, Petters and Kreidenweis[3] proposed a single parameter representation of a_w in terms of how the ratio of volume of solute (V_s) to the volume of water (V_w) affects a_w:

$$a_w = \left(1 + \kappa\frac{V_s}{V_w}\right)^{-1} \qquad (3)$$

Thus, in terms of the volume equivalent diameter of the hydrated particle (D) and of the dry solute (D_d), eq. 1 can be written as:

$$S(D) = \frac{D^3 - D_d^3}{D^3 - D_d^3(1-\kappa)}\exp\left(\frac{A}{D}\right) \qquad (4)$$

The parameter κ can be measured from a variety of experiments and predicts a given solute's effect on water uptake. In the sub-saturating regime, for example, one can rearrange eq. 3 to obtain the effect of κ on hygroscopic growth factor, *gf*, which is the ratio D/D_d, as a function of relative humidity (RH):

$$RH = \frac{gf^3 - 1}{gf^3 - (1-\kappa)} \exp\left(\frac{A}{D_d gf}\right) \quad (5)$$

Based on Raoult's law, a physical interpretation of κ can be derived from the definition of an ideal solution, where the activity of water is simply the mole fraction of water:

$$a_w = x_w = \frac{n_w}{n_w + n_s} \quad (6)$$

Noting that the number of moles can be expressed as the ratio of volume (V_i) to partial molar volume ($\overline{V}_i$) of the components, one obtains

$$a_w = \frac{V_w/\overline{V}_w}{V_w/\overline{V}_w + \upsilon V_s/\overline{V}_s} = \frac{1}{1 + \upsilon \frac{\overline{V}_w V_s}{\overline{V}_s V_w}} \quad (7)$$

where υ is the number of ions into which a solute can dissociate. Thus, the expression for a_w in eq. 3 represents the ideal limit where

$$\kappa^{ideal} \equiv \upsilon \frac{\overline{V}_w}{\overline{V}_s} \quad (8)$$

An optimistic approach then, would be to determine κ^{ideal} from the molar volume of the solute and water (Figure 1). This simplistic approach obtains the experimentally observed trend that larger solutes that do not dissociate are less hygroscopic (smaller κ), but it cannot be used in any quantitatively accurate way and fails to explain what has been described as "humidity-dependent hygroscopicity", where the measured value of κ is not a constant of humidity.[10]

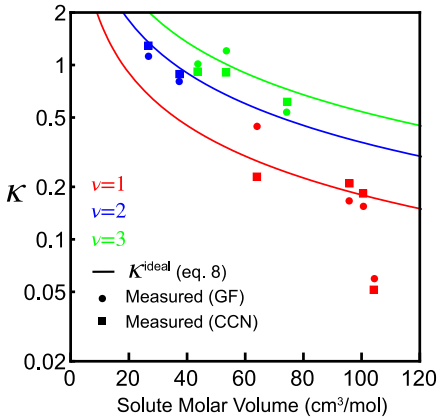

Figure 1: Predicted and measured hygroscopicity parameter (κ) as a function of the solute molar volume according to eq. 8, where υ=1, 2 and 3 represents the number of ions into which a solute can dissociate. Measured values are those compiled from ref. [3]. based on subsaturation growth factors (GF) or supersaturation cloud condensation nuclei (CCN) activation.

The limited accuracy displayed in Figure 1 may come from multiple sources. For example, the molar volume of a solute (or of water) is not necessarily equal to its partial molar volume in solution and ions may not completely dissociate to the expected value of υ. Since many factors can contribute to deviations from κ^{ideal}, using κ as an adjustable empirical parameter is a reasonable approach to approximate an ideal aerosol, particularly when the specific solute species are unknown. But if measured κ substantially differs from what one expects from eq. 8, the approximation of an ideal aerosol loses some appeal. It loses even more appeal when κ differs substantially based on how it is measured. If we could truly approximate hygroscopic aerosols as ideal aerosols, Figure 1 might look better.

Non-ideal aerosols

Returning to the definition of activity, missing from eq. 5, of course, is an activity coefficient, which accounts for deviations from ideal behavior:

$$a_w = \gamma_w x_w \qquad (9)$$

A convenient expression for the activity coefficient is that derived by Scratchard and Hildebrand,[11] in terms of the volumes of the solution's components:

$$RTln(\gamma_w) = \overline{V}_w \varphi_s^2 (\delta_w - \delta_s)^2 \quad (10)$$

Where

$$\varphi_s = \frac{V_s}{V_s + V_w} \qquad (11)$$

δ_w and δ_s are "solubility parameters" that are proportional to the molar volume and heat of vaporization of the pure compounds:

$$\delta_i = \sqrt{\frac{\Delta H_{vap} - RT}{\bar{V}_i}} \qquad (12)$$

Collecting the constants of eq. 10 into a single parameter, *B*, one obtains:

$$\gamma_w = exp\left[B\left(\frac{V_s}{V_s + V_w}\right)^2\right] \qquad (13)$$

where

$$B = \frac{\bar{V}_w(\delta_w - \delta_s)^2}{RT} \qquad (14)$$

While B has this derived meaning, we suggest it as an empirically adjustable parameter, akin to standard use of κ. Substituting diameters for volumes in eq. 13 and combining with eq. 4 yields an expression for the behavior of non-ideal aerosols that is an extension of κKT:

$$S(D) = \frac{D^3 - D_d^3}{D^3 - D_d^3(1-\kappa)} exp\left[B\left(\frac{D_d^3}{D^3}\right)^2\right] exp\left(\frac{A}{D}\right) \qquad (15)$$

By necessity, the expression for non-ideal aerosols is more cumbersome than that for ideal aerosols. Still, this expression is a simplification of the expression obtained in ref. [6] for non-ideal aerosols based on the Margules model for an activity coefficient. Here, we have a single additional parameter, *B*. Furthermore, by exploring limits of eq. 15, we can find realms where the parameters

B and κ are likely to be more or less important. First, there is a difference in the diameter-dependence of the ideal and non-ideal components of eq. 15. As the particle's size increases by absorbing more water, both factors approach unity, which is expected since $a_w \rightarrow 1$ at the limit of infinite dilution. The non-ideal factor dissipates more quickly, though, as D^6, versus D^3 for the ideal factor. Thus, non-ideal mixing will be most important where the solute is most concentrated, at low humidities and low growth factors. Furthermore, since κ is, in principle, an indicator of the solute's molar volume (eq. 8), κ will be smallest for large solutes, such as large organic compounds or polymers. In those cases, the ideal factor of eq. 15 will approach unity and the non-ideal component may dominate the aerosol's behavior. Additionally, the definition of B in terms of solubility parameters indicates that B will be most important for solutes with properties (i.e. ΔH_{vap} and $\overline{V}$) that differ from those of water.

Together, then, one expects the ideal component of eq. 15 to dominate for small polar solutes at high humidity, but for large non-polar solutes at low humidity, the non-ideal component will dominate (we confirm this below). This indeed may be the reason why κKT appears to succeed for salts but is more limited in its ability to describe organic-containing aerosols.[7, 9, 10] The functional form of the dominant term in eq. 15 differs for salts and organics. Thus, if one measures a subsaturation growth factor for a salt, κKT (the limit of $B \rightarrow 0$) is effective at predicting CCN activation. Simple κKT is ineffective at extrapolating to CCN activation for an organic solute, though; for such solutes, the non-ideal portion of eq. 15 will be more effective (the limit of $\kappa \rightarrow 0$). We explore these limits and realms of applicability further in attempting to interpret the results of MD simulations.

Computational Methods

At its root, hygroscopicity is a measure of the free energy of condensing water onto a particle: given a certain humidity, is it favorable or unfavorable for water to be in the condensed phase? With this in mind, we used free energy simulations to compute the chemical potential of water (μ_w), which is equal to the free energy of adding a water molecule to a particle ($\mu_w = \frac{\partial G}{\partial N_w}$). Through the relationship between μ_w and a_w, one can show that for a non-ideal aerosol, based on eq. 15

$$\frac{\mu_w}{RT} = B(1 + \frac{V_w}{V_s})^{-2} - ln\left(1 + \kappa\frac{V_s}{V_w}\right) \quad (16)$$

In the case of an ideal aerosol, $B \rightarrow 0$ and the first term disappears, yielding the equivalent equation for an ideal aerosol in κKT:

$$\frac{\mu_w}{RT} = -ln\left(1 + \kappa\frac{V_s}{V_w}\right) \quad (17)$$

Thus, our strategy was to calculate μ_w as a function of $\frac{V_s}{V_w}$ to determine either κ or B. Our general procedure for free energy simulations followed the method described by Shirts et al,[12] with some adaptations to the setting of aerosol particles with high solute concentrations. We used the program CHARMM[13, 14] to create particles of 5 nm diameter, which were mixtures of water and various solutes at a wide range of concentrations. The particles generally contained 6000-7000 atoms. We took care to maintain similar total volumes for the various particles, but the challenge of maintaining identical volume—and perhaps more crucially, identical surface area—for particles of such varied contents may explain some of the noise that ultimately appears in the results. The water in the simulations was modeled with a modified TIP3P force field[15] and the solutes used the CHARMM36 force field.[16-18]

Simulations were done using OpenMM 7.[19] Following a short energy minimization, the aerosols were heated from 48 K to 298 K during 1 ns using 1 fs time steps. A light harmonic restraint at the outer radius of the particle prevented evaporation, but otherwise the particles were surrounded by vacuum. The particles equilibrated at 298 K for 10 ns, at which point the free energy perturbation procedure[12, 20] started. The free energy perturbation method used the coupling factor λ to vary the strength of interactions between some given water molecule and the rest of the aerosol. The potential energy function, *U*, is parameterized, therefore, as:

$$U(\lambda) = U_{N_w - 1} + \lambda(U_{N_w} - U_{N_w - 1}) \quad (18)$$

Where N_w is the number of water molecules and λ varies from 0 to 1. One can then obtain the free energy of adding a water molecule by decoupling the water during simulations at a range of λ and finding the ensemble averaged derivative of energy with respect to λ:

$$\frac{\partial G}{\partial N_w} = \int_0^1 \frac{\partial G(\lambda)}{\partial \lambda} d\lambda = \int_0^1 \left\langle \frac{\partial U(\lambda)}{\partial \lambda} \right\rangle_\lambda d\lambda \qquad (19)$$

The decoupling simulations occurred in two stages, first for electrostatic interactions and then for van der Waals interactions. A soft-core potential[21] for the van der Waals interactions avoided numerical instability near $\lambda = 0$. The simulations were equilibrated at each value of λ for 100 ps followed by production runs of 5 ns where $\frac{\partial U(\lambda)}{\partial \lambda}$ was calculated every 100 fs. Simulations at one value of λ were used to seed the simulation at the next value of λ. 11 values of λ were used for electrostatics and 17 values were used for van der Waals. For each particle, this decoupling procedure was used for at least 5 different randomly chosen water molecules and the final results represent the averages of all the water molecules examined. We integrated $\left\langle \frac{\partial U(\lambda)}{\partial \lambda} \right\rangle_\lambda$ numerically and estimated statistical uncertainty in $\left\langle \frac{\partial U(\lambda)}{\partial \lambda} \right\rangle_\lambda$ from block averaging of individual simulations.

Results and Discussion

We have calculated the chemical potential of water, μ_w, as a function of V_s/V_w for the highly hygroscopic salts NaCl and $(NH_4)_2SO_4$ (Ammonium sulfate, AS). We find the expected trend for hygroscopic solutes: μ_w decreases as more solute is added, meaning that a higher fraction of solute makes the addition of water more favorable (Figure 2). The data from the MD simulations are somewhat noisy relative to the magnitude of change in μ_w induced by increases in V_s/V_w. These magnitudes appear to be near the limit of what MD simulations can reliably detect. To test models of hygroscopicity, we fitted the data to both eq. 16 and eq. 17. In eq. 17, which represents κKT, we used κ as the fitting parameter. This yields $\kappa_{NaCl}^{MD} = 1.51 \pm 0.49$ and $\kappa_{AS}^{MD} = 2.20 \pm 0.35$. The value for NaCl is within error of experimentally measured values ($\kappa_{NaCl}^{exp} = 1.1 - 1.3$), but the value for AS is significantly larger than experiments have measured ($\kappa_{AS}^{exp} = 0.5 - 0.6$).

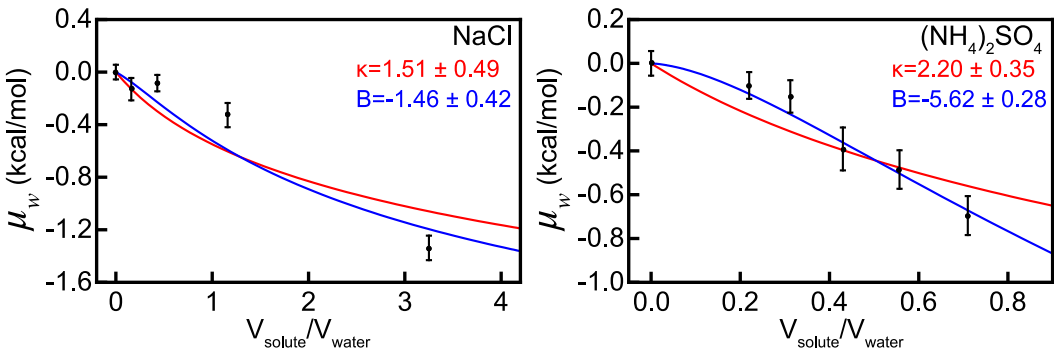

Figure 2: Calculated μ_w as a function of V_s/V_w for inorganic salts. The fitted lines are to the models for ideal κKT (red, eq. 17) and non-ideal κKT (blue, eq. 16). The model for ideal behavior uses κ as the fitting parameter. In order to maintain a single fitting parameter in the model for non-ideal behavior, that model assumed a value of κ based on solute properties using eq. 8 ($\kappa_{NaCl}^{ideal} = 1.34$; $\kappa_{AS}^{ideal} = 0.72$) and used B as the sole fitting parameter. The noise in the data from the MD simulations makes it challenging to distinguish between these models based on goodness-of-fit criteria. A model using the functional form for ideal mixing appears to be a reasonable approximation to these data, although the fitted parameter, κ, differs somewhat from κ^{ideal} as well as from values determined experimentally ($\kappa_{NaCl}^{exp} = 1.1 - 1.3$; $\kappa_{AS}^{exp} = 0.5 - 0.6$). Error bars represent propagation of statistical uncertainties from block averaging of individual simulations.

The calculated differences versus the experimental data could arise from a number of sources. The force field parameters for the solutes, as well as water, are developed for environments and goals that dramatically differ from how we have used them here. To our knowledge there are no MD force fields that have been developed to model systems such as these with extremely high salt concentrations. For example, typical biological simulations use NaCl concentrations of around 150 mM, which is orders of magnitude more dilute than our simulations: $\frac{V_s}{V_w} = 1$ corresponds to an almost comical concentration of 18.6 M NaCl. Furthermore, the force fields are typically parameterized to simulate bulk using periodic boundary conditions; our simulated aerosols are surrounded by vacuum. In addition to the hazards of applying force fields to unintended environments, the extremely high salt concentrations limit the rate of diffusion through the aerosols, which hinders the efficiency of MD sampling. We used many replicates, choosing as many as 30-40 different water molecules for some setups, in order to sample their different conformations and environments. Still, some noise and inaccuracy resulting from slow diffusion is unavoidable.

Finally, potential sources of discrepancy versus experiment lie in the particular aerosol models that we have simulated. First, they are quite small, with hydrated diameter $D = 5\ nm$, whereas experiments typically probe aerosols with dry diameters D_d on the order of 100s of nm to

microns. Furthermore, the range of $\frac{V_s}{V_w}$ that the simulations have examined differs somewhat from the range typically amenable to experimental measures. $\frac{V_s}{V_w} = 1$ corresponds to a growth factor of 1.26, whereas CCN activation typically occurs at much more hydrated ranges. In order to detect changes in μ_w the simulations must focus on relatively dry particles. In principle, however, these last two potential sources of discrepancy—the difference in size and water content in the simulations vs. experiment—should not play any role. As defined in κKT the value of κ is independent of the size of an aerosol particle or its water content. Thus, if these factors *do* play a role,[6, 8-10, 22] they expose a limitation in κ as a measure of hygroscopicity. We explore the possible limitations as resulting from *non-negligible* contributions from non-ideal mixing.

To test the possible role of non-ideal behavior, we fitted the data for μ_w vs. V_s/V_w to eq. 16 using B as a fitting parameter (Figure 2). One could use both B and κ as fitting parameters, which would presumably yield a better fit to the data, but the limits of the data do not warrant two independent fitting parameters. Thus, in order to preserve the goal of a single hygroscopicity parameter we set $\kappa = \kappa^{ideal}$ (cf. eq. 8), leaving B as the only fitting parameter. For the salts in Figure 2, the model for non-ideal behavior does not appear to offer any obvious advantages over that for ideal κKT: both curves pass through the data points as well as can be expected given the noise in the data. Both solutes exhibit a negative deviation from Raoult's law and the larger magnitude of B for AS vs. NaCl (B_{AS}=-5.62 ± 0.28 and B_{NaCl}=-1.46 ± 0.42) indicates that AS mixing with water is less ideal than NaCl. If the non-ideal behavior implied by these fits is "real" it would suggest that experiments would yield different values of κ if they measured hygroscopic growth at different humidities. We explore this more below in the context of ideal and non-ideal Köhler curves. First, though, we turn to the question of organic solutes, which have proven a particular challenge to the predictive capabilities of κKT.[6-10]

Using analogous methods to the simulations of salts, we calculated μ_w as a function of V_s/V_w for isopropanol (iPrOH) and glucose (Figure 3). In these cases, the surprising result is that μ_w *increases* as V_s/V_w increases, meaning additional solute makes adding water *less* favorable. While this trend is counter to that expected based on the hygroscopic salts in Figure 2, the fact that these solutes make the addition of water less favorable is not unreasonable: this is simply the hydrophobic effect. In terms of interpreting this result in the context of κKT, however, increasing μ_w as a function of V_s/V_w results in non-physical values of κ. One can fit the data to eq. 17, but

the only way for μ_w to increase as a function of V_s/V_w is for κ to be less than 0. $\kappa < 0$ leads to a number of problems: it implies that $\mu_w \to \infty$ as $\kappa\frac{V_s}{V_w} \to -1$. In the case of the fit to glucose, for example, where $\kappa = -0.25$, μ_w becomes undefined for a particle where $\frac{V_s}{V_w} = 4$. Furthermore, when one attempts to use negative values of κ to predict hygroscopic growth and CCN activation in eqs. 4-5, one obtains non-sensical results, such as growth factors less than 1. Clearly something is missing in the modeling of these organic solutes and accounting for non-ideal behavior offers a solution.

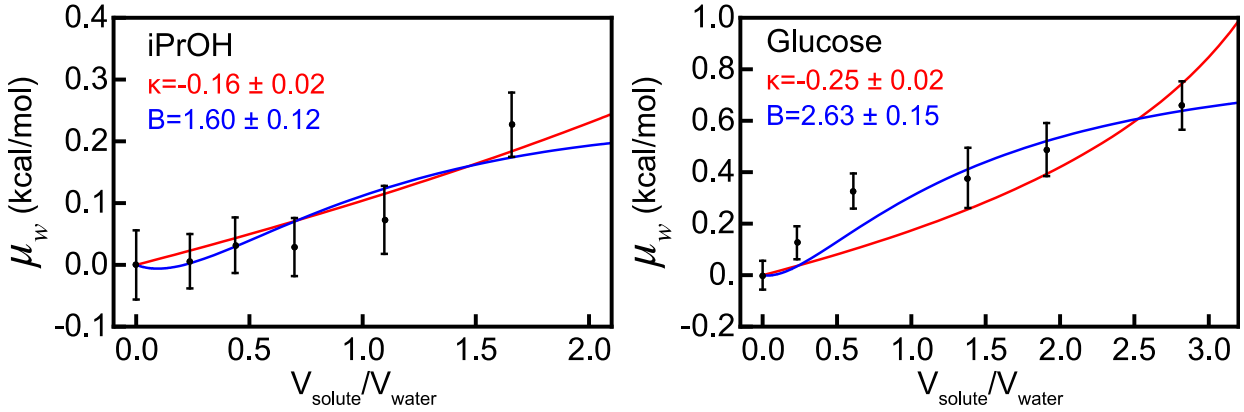

Figure 3: Calculated μ_w as a function of V_s/V_w for organic solutes. The fitted lines are to the models for κKT (red) and non-ideal κKT (blue). The model for ideal behavior uses κ as the fitting parameter in eq. 17. In order to maintain a single fitting parameter in the model for non-ideal behavior, that model assumed a value of κ based on solute properties ($\kappa_{iPrOH}^{ideal} = 0.24$ and $\kappa_{Glucose}^{ideal} = 0.15$; cf. eq. 8) and used B as the sole fitting parameter in eq. 16. The fact that fits to eq. 17 yield $\kappa < 0$ indicate that κKT is inadequate for describing these results. The fits to a model of non-ideal behavior yield physically sound behavior within the expected (limited) accuracy of this kind of modeling.

As described above, non-ideal behavior ought to make a larger contribution to the mixing of larger and less polar solutes. Here we see that non-ideal mixing is actually the dominant effect in total μ_w. While neither iPrOH nor glucose is particularly large, they are both less polar than water and this is revealed in the striking deviation from ideal behavior evident in Figure 3. In contrast to the salts above, which yielded $B < 0$, the organic solutes result in $B > 0$. This difference in the direction of the non-ideal component is a reflection of either positive or negative deviation from Raoult's law—an activity coefficient greater than or less than unity. This positive deviation from Raoult's law cannot be accommodated by an empirical adjustment of κ in ideal κKT (or, for that matter, by the analogous single-parameter model of ref. [23] using ρ_{ion}). In both cases of organics, $\mu_w > 0$ for nearly the entire range of dilutions, which indicates that the excess free energy

of mixing outweighs the ideal entropy of mixing. Thus, non-ideal mixing is the dominant effect in subsaturation hygroscopicity for these organic aerosols. This breakdown of idealized single-parameter models for activity may explain some of the discrepancies observed when κ is measured for organic solutes across large regions of humidity.[6-9]

Ideal and Non-ideal Köhler Curves

The non-ideal factor of eq. 15 is a different functional form (an exponential) from the ideal factor. Thus, aerosols that are dominated by non-ideal behavior, such as the organic aerosols just discussed, will yield Köhler curves that are a different shape than those dominated by ideal behavior. In the case of the fits to salts, where the non-ideal behavior is a negative deviation from Raoult's law ($B < 0$) the result is surprisingly steep growth at low humidity but shallower growth as the solute becomes more diluted at higher humidities (Figure 4). That is, for a solute with a given growth factor measured at subsaturation humidity, a negative deviation from Raoult's law indicates that S_c could be larger than that predicted by κKT. For example, using the parameters for NaCl obtained from the MD simulations we obtain ideal and non-ideal Köhler curves that intersect at around RH=35% (Figure 4A, red dashed and red dotted lines). As humidity increases, the curve for non-ideal growth (dotted) increases more slowly and results in a S_c (the maximum of the curve in panel 4B) around 0.15, vs. 0.1 for ideal growth. As discussed above, the different concentration dependence of ideal versus non-ideal behavior means non-ideal behavior will play a larger role at lower humidity. In this case, the negative deviation from Raoult's law yields more growth at low humidity. At higher humidity, the ideal component is more pronounced. Since the curves for non-ideal growth used the values of κ derived from molecular volume, and those values are smaller than the values fitted to the model of ideal mixing, the shallower growth at higher humidity and the ultimately larger S_c reflects this smaller value of κ. As discussed below, if one uses identical values of κ, but varies B, the behavior at large D (including the value of S_c) is insensitive to the value of B.

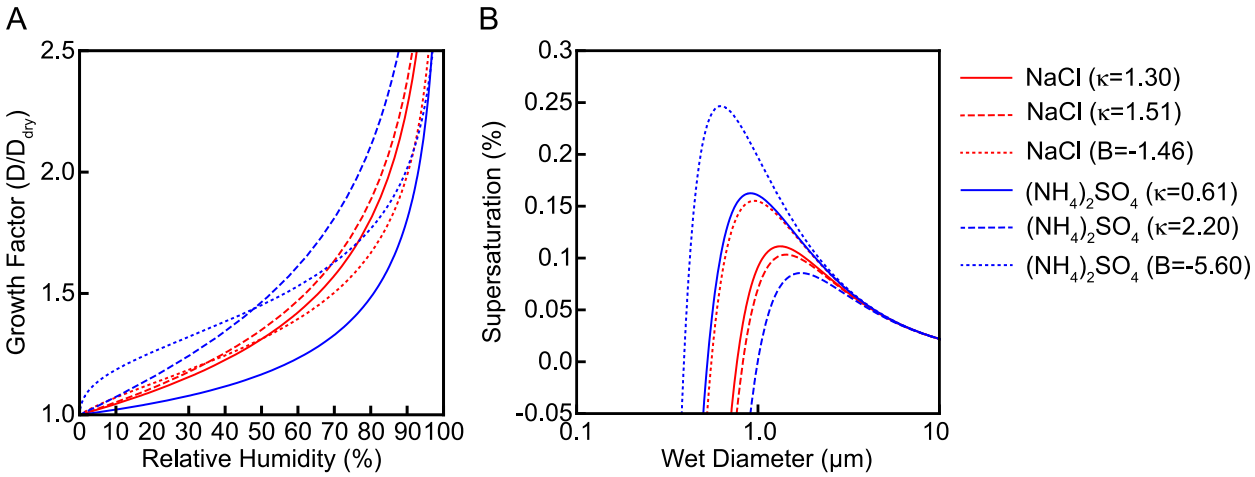

Figure 4: Köhler curves at subsaturating (A) and supersaturating (B) humidities for particles with dry diameter (D_d) of 100 nm. For both NaCl and $(NH_4)_2SO_4$, the solid line corresponds to κKT (eq. 4) with the experimentally determined value of κ. The dashed line is ideal κKT with the value of κ fitted from MD simulations. The dotted lines are the curves for non-ideal aerosols (eq. 15) using the parameters fitted from MD simulations. Depending on the magnitude and direction of the non-ideal behavior, the shape of the growth curves can deviate substantially from the expected growth and CCN activation based on ideal behavior.

The growth curves based on the parameters obtained for the organic solutes (Figure 5), which have dominating positive deviations from Raoult's law, differ substantially from typical Köhler curves. The positive deviation from Raoult's law results in suppressed growth factors at low humidity, including as humidity approaches saturation conditions. The truly surprising behavior occurs at supersaturation conditions, though, where an extraordinarily large S_c (ca. 250%) is necessary to activate glucose. This is obviously not an accurate model of glucose, based on the experimentally observed activation.[24] This is a shortcoming of the force field parameters from the MD simulations, but there is nothing physically unreasonable about an aqueous solution with a large positive deviation from Raoult's law. Perhaps even more intriguing than the results for glucose, though, are those for iPrOH which has a more modest positive deviation from Raoult's law (B=1.60 for iPrOH, vs. B=2.63 for glucose). In the case of iPrOH, there is not a *single* S_c, but rather there are two local maxima in the Köhler curve. The first, like glucose, occurs at a quite large supersaturation ($S_{c1} \approx$ 50%) but the second occurs at a value more typically expected ($S_{c2} \approx$ 0.25%, Figure 5B, inset). Similarly, the curve for glucose contains a "shoulder" in the vicinity of the S_c expected for an ideal aerosol with $\kappa = 0.16$. Analogous to the salts above, the complex behavior of these curves can be understood in terms of the regions where ideal and non-ideal behavior make important contributions. As noted, the non-ideal component is most important at high solute concentration. It is here, at high solute concentrations, that positive deviations from

Raoult's law can so substantially increase the supersaturation. As the particle grows and the solute becomes more dilute, the non-ideal contributions to activity dissipate faster than the ideal contributions and the curves approach the limit of κKT. Importantly, the curve for iPrOH makes a novel, testable prediction for the region where $0 < S < S_{c2}$: whereas ideal κKT predicts two possible diameters for equilibrated particles in this region, our model indicates that four diameters are possible for certain types of aerosols with positive deviations from Raoult's law.

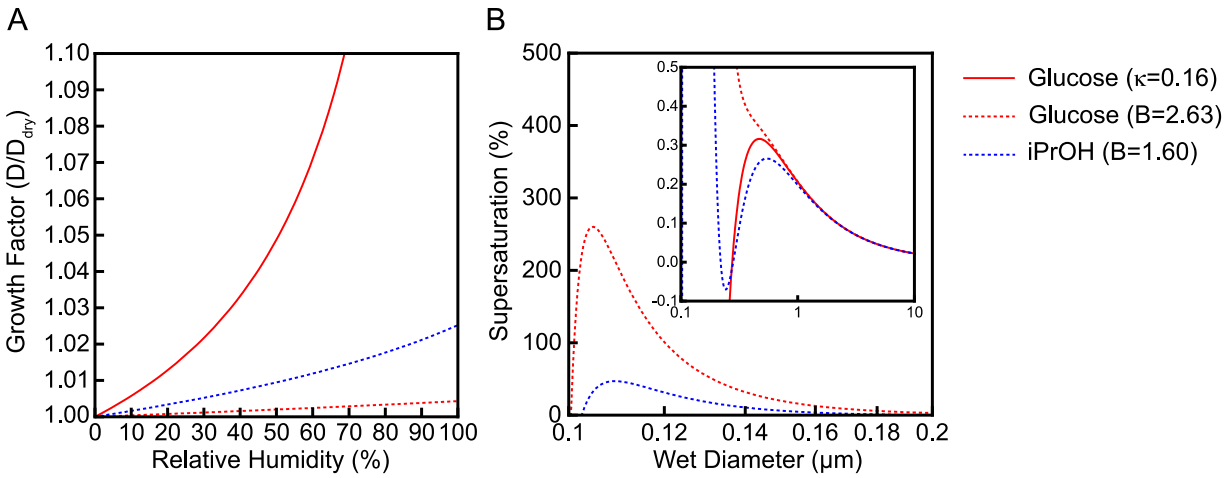

Figure 5: Köhler curves at subsaturating (A) and supersaturating (B) humidities for particles with dry diameter (D_d) of 100 nm. For glucose, the solid line corresponds to κKT (eq. 4) with the experimentally determined value of κ (an experimental value for iPrOH is not available, to our knowledge). The dotted lines are the curves for non-ideal aerosols (eq. 15) using the parameters fitted from MD simulations. Since the MD simulations implied values of $\kappa < 0$ we cannot present corresponding curves for ideal κKT. The inset of part B shows that a second S_c occurs in the curve for iPrOH, which is near the S_c expected for an ideal aerosol with modest hygroscopicity.

The intriguing effects of deviations from ideal behavior in Figures 4 and 5 inspired us to explore the Köhler curves of hypothetical solutes with more modest deviations from Raoult's law (Figure 6). What we find is that small deviations from ideal mixing can have important effects on subsaturation growth while yielding indistinguishable behavior near the critical supersaturation. Positive deviations from ideality suppress subsaturation growth while negative deviations enhance subsaturation growth. Experimentally, then, if one measured subsaturation growth factors for a solute with positive deviation from ideal behavior, but then used ideal κKT to predict CCN activation, the predicted S_c would be too large.[6-10] The effects of the positive deviation from ideal behavior dissipate as the solute becomes more dilute and S_c is lower than ideal κKT would predict. This behavior, namely higher CCN activity than expected based on growth factors, has been observed as the "hygroscopicity gap" and has been in need of an explanation for some time.[6-10]

We hope the flexibility of the model proposed here, which can accommodate both positive and negative deviations from Raoult's law with a single additional parameter, will aid the development of predictive models for real aerosol behavior.

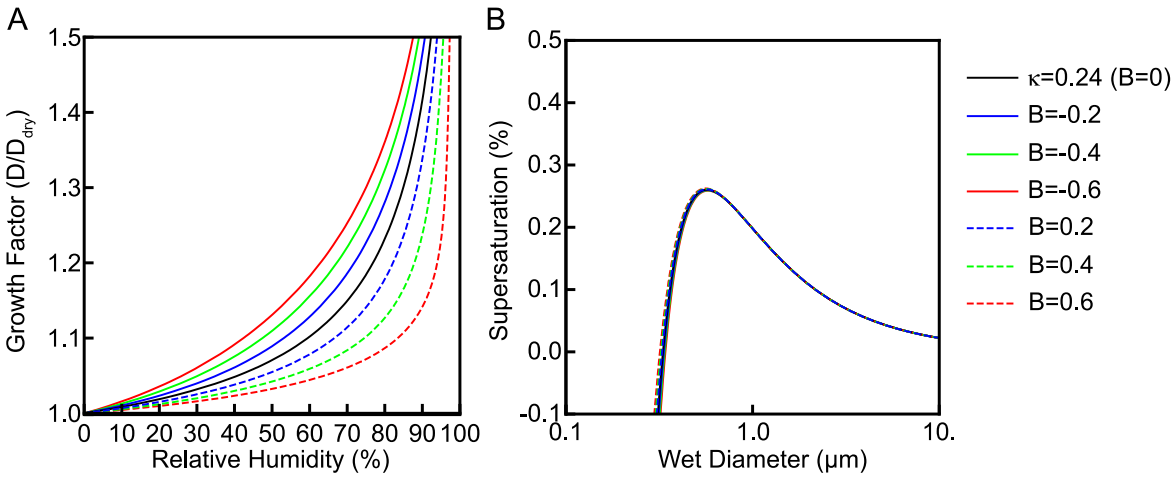

Figure 6: Köhler curves at subsaturating (A) and supersaturating (B) humidities for a hypothetical solute with D_{dry}=100 nm, molar volume equivalent to iPrOH ($\kappa^{ideal} = 0.24$), and with varying contributions from non-ideal mixing. Non-ideal mixing can suppress or enhance growth at low humidity without altering the CCN activity. This results from the fact that non-ideal behavior contributes more to the curves at high solute concentration (low D in eq. 15) and its effects dissipate quickly as D increases.

Other work toward closing the hygroscopicity gap has emphasized another important component of κKT, namely the surface tension (σ) that appears in the Kelvin term (eqs. 1-2). A typical approximation is to use the surface tension of pure water, but this approximation may be misleading for some solutes, particularly at high concentrations.[7] Both non-ideal mixing and altered surface tension will be most important in particles with high solute concentration and additional study will need to determine when and how to include these effects in the most useful manner.

In terms of practical significance for atmospheric science, an unfortunate consequence of a two-parameter model, whether the additional parameter accounts for non-ideal mixing or for changes in surface tension, is that a single data point does not uniquely define the model. To obtain precise values for κ and for B one must measure growth factors and activation across a range of relative humidity. A possible solution to this problem is to reduce the empirical portion of the non-ideal model by assuming $\kappa = \kappa^{ideal}$ (as we did in our fits to the MD results) and thus only B needs to be measured for a given solute. In principle B can be measured at a single humidity, but that humidity should be as low as possible, where non-ideal mixing contributes most. If, on the other

hand, the molecular composition of an aerosol is not known, κ^{ideal} cannot be approximated from molar volume and both parameters must ultimately be measured. The fact that modest amounts of non-ideal mixing—particularly negative deviations from Raoult's law—contribute little to S_c (Figure 6) indicates that in some cases S_c can still be used as a single measurement approximation of κ, but caution must be exercised in predictions of subsaturation growth based upon measurements of S_c alone. Furthermore, if a solute exhibits large positive deviation from Raoult's law, the observed S_c could be drastically different from that expected for ideal mixing (Figure 5).

Conclusions

We have used molecular dynamics simulations and free energy perturbation to model hygroscopicity for salts and organic solutes based on the chemical potential of water. We find that the simulations are not quantitatively accurate, owing to the subtle changes in chemical potential induced by solutes. Force field parameters are not optimized for this goal and are meant for environments with far lower solute concentrations. Nonetheless, the simulations serve as proof of principle that, given an appropriate force field, hygroscopicity can be modeled and predicted through these methods. As MD simulations become more widely applied to aerosol chemistry,[25-28] it may be worthwhile to develop specific force fields for these applications rather than adopting biological force fields for such extreme environments.

While the simulations are not quantitatively accurate, they allow us to qualitatively evaluate the framework of κKT. We find that non-ideal mixing of solute and water can sometimes pose an insurmountable challenge to κKT. By adding an activity coefficient term to κKT we are able to account for this non-ideal behavior and we find that small contributions from non-ideal mixing can result in important changes in the overall shape of Köhler curves. This change in shape means that a measured growth factor at subsaturation humidity may be misleading about CCN activation at supersaturation humidity.

Much of κKT's success has stemmed from the fact that it requires just a single parameter and parsimony is, of course, a worthwhile pursuit. In principle, this allows a single measurement, of either growth factor or S_c to allow comparisons and predictions of the behavior of different aerosols. But so-called humidity-dependent hygroscopicity[10] reveals a flaw in this notion. Unfortunately, if κ differs under different humidity or for different dry particle sizes, then assigning a value of κ to some aerosol offers no more insight than is offered by the raw growth

factors or S_c. The primary advantages of κKT are that it affords a simple metric for comparing aerosols of unknown contents and that it yields simple mixing rules for multi-component aerosols. But if κ is not, in general, constant for a particular solute or aerosol, then it loses utility for comparison among aerosols: aerosol A could be more hygroscopic than aerosol B today and less hygroscopic tomorrow. If hygroscopicity is a property of an aerosol itself, and not any environmental factors, then κ alone is not a good measure of hygroscopicity. A "hygroscopicity constant" ought to be just that—constant.

A model that accounts for non-ideal behavior is necessarily more complicated than one that assumes ideal behavior. Nonetheless, it should surprise nobody that mixtures of water, with its unique intermolecular interactions, can yield highly non-ideal solutions. The occasional inaccuracy of κKT, particularly exemplified by the so-called "hygroscopicity gap", suggests that a single parameter is often insufficient.[4-10] Our model for non-ideal behavior contains two parameters, κ and B, which is what yields its greater flexibility than a model with only κ. Our simulations showed that non-ideal mixing is particularly pronounced in the case of organic solutes; this may be due in part to inaccuracies in the MD force field parameters, but the definitions of κ^{ideal} and B suggest it will generally be true that large organic species exhibit more pronounced non-ideal behavior. The practical importance of an extension of κKT for non-ideal behavior is substantial in these cases because such behavior cannot be accounted for by an empirical adjustment of κ. The functional form for hygroscopic growth differs when that growth is due substantially to non-ideal mixing.

By approaching the problem of hygroscopicity from an untested direction, namely free energy simulations, we have uncovered useful insights into the phenomenon and made new, testable predictions about possible particle sizes at supersaturation humidity. The novel class of data from MD simulations places large restrictions on the possible form of a general theory of hygroscopic growth and CCN activation. The results show that for some particles, excess free energy of mixing will dominate overall hygroscopicity and ignoring non-ideal mixing will be perilous. We hope future interpretations of experimental results and further developments of models will consider the importance of non-ideal mixing.

Conflicts of Interest

There are no conflicts of interest to declare.

Acknowledgements

The author is grateful to Vicki H. Grassian for fruitful discussions and useful comments on a draft of the manuscript. This work was supported by the National Science Foundation through the Center for Aerosol Impacts on Chemistry of the Environment (CAICE), an NSF funded Center for Chemical Innovation (CHE-1801971). Computational resources were provided by the NSF through an XSEDE allocation (TG-CHE060073N) and by the lab of Rommie E. Amaro.

References

1. Seinfeld, J. H.; Pandis, S. N., *Atmospheric Chemistry and Physics*. 2nd Ed. ed.; John Wiley & Sons, inc: Hoboken, New Jersey, 2006.
2. Stadnytskyi, V.; Bax, C. E.; Bax, A.; Anfinrud, P., The airborne lifetime of small speech droplets and their potential importance in SARS-CoV-2 transmission. *Proceedings of the National Academy of Sciences* **2020**, 202006874.
3. Petters, M. D.; Kreidenweis, S. M., A single parameter representation of hygroscopic growth and cloud condensation nucleus activity. *Atmospheric Chemistry and Physics* **2007,** *7* (8), 1961-1971.
4. Petters, M. D.; Kreidenweis, S. M., A single parameter representation of hygroscopic growth and cloud condensation nucleus activity - Part 2: Including solubility. *Atmospheric Chemistry and Physics* **2008,** *8* (20), 6273-6279.
5. Petters, M. D.; Kreidenweis, S. M., A single parameter representation of hygroscopic growth and cloud condensation nucleus activity - Part 3: Including surfactant partitioning. *Atmospheric Chemistry and Physics* **2013,** *13* (2), 1081-1091.
6. Petters, M. D.; Wex, H.; Carrico, C. M.; Hallbauer, E.; Massling, A.; McMeeking, G. R.; Poulain, L.; Wu, Z.; Kreidenweis, S. M.; Stratmann, F., Towards closing the gap between hygroscopic growth and activation for secondary organic aerosol - Part 2: Theoretical approaches. *Atmospheric Chemistry and Physics* **2009,** *9* (12), 3999-4009.
7. Forestieri, S. D.; Staudt, S. M.; Kuborn, T. M.; Faber, K.; Ruehl, C. R.; Bertram, T. H.; Cappa, C. D., Establishing the impact of model surfactants on cloud condensation nuclei activity of sea spray aerosol mimics. *Atmospheric Chemistry and Physics* **2018,** *18* (15), 10985-11005.
8. Poulain, L.; Wu, Z.; Petters, M. D.; Wex, H.; Hallbauer, E.; Wehner, B.; Massling, A.; Kreidenweis, S. M.; Stratmann, F., Towards closing the gap between hygroscopic growth and CCN activation for secondary organic aerosols - Part 3: Influence of the chemical composition on the hygroscopic properties and volatile fractions of aerosols. *Atmospheric Chemistry and Physics* **2010,** *10* (8), 3775-3785.
9. Wex, H.; Petters, M. D.; Carrico, C. M.; Hallbauer, E.; Massling, A.; McMeeking, G. R.; Poulain, L.; Wu, Z.; Kreidenweis, S. M.; Stratmann, F., Towards closing the gap between

hygroscopic growth and activation for secondary organic aerosol: Part 1-Evidence from measurements. *Atmospheric Chemistry and Physics* **2009,** *9* (12), 3987-3997.

10. Liu, P. F.; Song, M. J.; Zhao, T. N.; Gunthe, S. S.; Ham, S. H.; He, Y. P.; Qin, Y. M.; Gong, Z. H.; Amorim, J. C.; Bertram, A. K.; Martin, S. T., Resolving the mechanisms of hygroscopic growth and cloud condensation nuclei activity for organic particulate matter. *Nat. Commun.* **2018,** *9*, 10.

11. Elliot, J. R.; Lira, C. T., *Introductory Chemical Engineering Thermodynamics*. Prentice Hall Inc.: Upper Saddle River, New Jersey, 1999.

12. Shirts, M. R.; Pitera, J. W.; Swope, W. C.; Pande, V. S., Extremely precise free energy calculations of amino acid side chain analogs: Comparison of common molecular mechanics force fields for proteins. *Journal of Chemical Physics* **2003,** *119* (11), 5740-5761.

13. Brooks, B. R.; Brooks, C. L.; Mackerell, A. D.; Nilsson, L.; Petrella, R. J.; Roux, B.; Won, Y.; Archontis, G.; Bartels, C.; Boresch, S.; Caflisch, A.; Caves, L.; Cui, Q.; Dinner, A. R.; Feig, M.; Fischer, S.; Gao, J.; Hodoscek, M.; Im, W.; Kuczera, K.; Lazaridis, T.; Ma, J.; Ovchinnikov, V.; Paci, E.; Pastor, R. W.; Post, C. B.; Pu, J. Z.; Schaefer, M.; Tidor, B.; Venable, R. M.; Woodcock, H. L.; Wu, X.; Yang, W.; York, D. M.; Karplus, M., CHARMM: The Biomolecular Simulation Program. *Journal of Computational Chemistry* **2009,** *30* (10), 1545-1614.

14. Brooks, B. R.; Bruccoleri, R. E.; Olafson, B. D.; States, D. J.; Swaminathan, S.; Karplus, M., CHARMM - A Program For Macromolecular Energy, Minimization, and Dynamics Calculations. *Journal of Computational Chemistry* **1983,** *4* (2), 187-217.

15. Jorgensen, W. L.; Chandrasekhar, J.; Madura, J. D.; Impey, R. W.; Klein, M. L., Comparison of Simple Potential Functions for Simulating Liquid Water. *Journal of Chemical Physics* **1983,** *79* (2), 926-935.

16. Guvench, O.; Greene, S. N.; Kamath, G.; Brady, J. W.; Venable, R. M.; Pastor, R. W.; Mackerell, A. D., Additive Empirical Force Field for Hexopyranose Monosaccharides. *Journal of Computational Chemistry* **2008,** *29* (15), 2543-2564.

17. MacKerell, A. D.; Bashford, D.; Bellott, M.; Dunbrack, R. L.; Evanseck, J. D.; Field, M. J.; Fischer, S.; Gao, J.; Guo, H.; Ha, S.; Joseph-McCarthy, D.; Kuchnir, L.; Kuczera, K.; Lau, F. T. K.; Mattos, C.; Michnick, S.; Ngo, T.; Nguyen, D. T.; Prodhom, B.; Reiher, W. E.; Roux, B.; Schlenkrich, M.; Smith, J. C.; Stote, R.; Straub, J.; Watanabe, M.; Wiorkiewicz-Kuczera, J.; Yin, D.; Karplus, M., All-atom empirical potential for molecular modeling and dynamics studies of proteins. *J. Phys. Chem. B* **1998,** *102* (18), 3586-3616.

18. Yoo, J.; Aksimentiev, A., Improved Parameterization of Amine-Carboxylate and Amine-Phosphate Interactions for Molecular Dynamics Simulations Using the CHARMM and AMBER Force Fields. *Journal of Chemical Theory and Computation* **2016,** *12* (1), 430-443.

19. Eastman, P.; Swails, J.; Chodera, J. D.; McGibbon, R. T.; Zhao, Y. T.; Beauchamp, K. A.; Wang, L. P.; Simmonett, A. C.; Harrigan, M. P.; Stern, C. D.; Wiewiora, R. P.; Brooks, B. R.; Pande, V. S., OpenMM 7: Rapid development of high performance algorithms for molecular dynamics. *Plos Computational Biology* **2017,** *13* (7).

20. Shirts, M. R.; Mobley, D. L., An Introduction to Best Practices in Free Energy Calculations. In *Biomolecular Simulations. Methods in Molecular Biology (Methods and Protocols)*, Monticelli, L.; Salonen, E., Eds. Humana Press: Totowa, NJ, 2013; Vol. 924.

21. Beutler, T. C.; Mark, A. E.; Vanschaik, R. C.; Gerber, P. R.; Vangunsteren, W. F., AVOIDING SINGULARITIES AND NUMERICAL INSTABILITIES IN FREE-ENERGY CALCULATIONS BASED ON MOLECULAR SIMULATIONS. *Chemical Physics Letters* **1994,** *222* (6), 529-539.
22. Laskina, O.; Morris, H. S.; Grandquist, J. R.; Qiu, Z.; Stone, E. A.; Tivanski, A. V.; Grassian, V. H., Size Matters in the Water Uptake and Hygroscopic Growth of Atmospherically Relevant Multicomponent Aerosol Particles. *Journal of Physical Chemistry A* **2015,** *119* (19), 4489-4497.
23. Wex, H.; Hennig, T.; Salma, I.; Ocskay, R.; Kiselev, A.; Henning, S.; Massling, A.; Wiedensohler, A.; Stratmann, F., Hygroscopic growth and measured and modeled critical super-saturations of an atmospheric HULIS sample. *Geophysical Research Letters* **2007,** *34* (2).
24. Chen, C. C.; Tao, C. J.; Cheng, H. C., Condensation of supersaturated water vapor on charged/neutral nanoparticles of glucose and monosodiurn glutamate. *Journal of Colloid and Interface Science* **2002,** *255* (1), 158-170.
25. Luo, M.; Dommer, A. C.; Schiffer, J. M.; Rez, D. J.; Mitchell, A. R.; Amaro, R. E.; Grassian, V. H., Surfactant Charge Modulates Structure and Stability of Lipase-Embedded Monolayers at Marine-Relevant Aerosol Surfaces. *Langmuir* **2019,** *35* (27), 9050-9060.
26. Schiffer, J. M.; Luo, M.; Dommer, A. C.; Thoron, G.; Pendergraft, M.; Santander, M. V.; Lucero, D.; de Barros, E. P.; Prather, K. A.; Grassian, V. H.; Amaro, R. E., Impacts of Lipase Enzyme on the Surface Properties of Marine Aerosols. *Journal of Physical Chemistry Letters* **2018,** *9* (14), 3839-3849.
27. Karadima, K. S.; Mavrantzas, V. G.; Pandis, S. N., Molecular dynamics simulation of the local concentration and structure in multicomponent aerosol nanoparticles under atmospheric conditions. *Physical Chemistry Chemical Physics* **2017,** *19* (25), 16681-16692.
28. Karadima, K. S.; Mavrantzas, V. G.; Pandis, S. N., Insights into the morphology of multicomponent organic and inorganic aerosols from molecular dynamics simulations. *Atmospheric Chemistry and Physics* **2019,** *19* (8), 5571-5587.